

1

Mucosal or systemic microbiota exposures shape the B cell repertoire

Hai Li ^{1*}, Julien P. Limenitakis ^{1*}, Victor Greiff ², Bahtiyar Yilmaz ¹, Olivier Schären ³, Camilla Urbaniak ⁴, Mirjam Zünd ¹, Melissa A.E. Lawson ¹, Ian D. Young ¹, Sandra Rupp ¹, Mathias Heikenwälder ⁵, Kathy D. McCoy ¹, Siegfried Hapfelmeier ³, Stephanie C. Ganal-Vonarburg ^{1*†}, Andrew J. Macpherson ^{1*†}

¹ Maurice Müller Laboratories (DBMR), Universitätsklinik für Viszerale Chirurgie und Medizin Inselspital, Murtenstrasse 35, University of Bern, 3008 Bern, Switzerland.

² University of Oslo, Dept. of Immunology, 0372 Oslo, Norway.

³ Institute for Infectious Diseases, University of Bern, 3001 Bern, Switzerland.

⁴ McMaster University Medical Centre, Hamilton, Ontario, Canada.

⁵ Division of Chronic Inflammation and Cancer, German Cancer Research Center (DKFZ), Heidelberg, Germany.

* These authors have made an equal contribution.

† Correspondence to: andrew.macpherson@dbmr.unibe.ch; stephanie.ganal@dbmr.unibe.ch

University Hospital Bern (Inselspital), D117, BHH, Bern 3010, Switzerland, Tel. +41 31 632 8025

2 **FIRST PARAGRAPH**

3 Microbiota colonization causes profound B cell stimulation and immunoglobulin induction, yet mammals
4 colonized with many taxa have highly complex individualized immunoglobulin repertoires^{1,2}. To
5 deconstruct how the microbiota shapes the B cell pool and its functional responsiveness we have used a
6 simplified model of defined transient microbial exposures by different taxa in germ-free mice³. B cell
7 immunoglobulin repertoire development was followed by deep sequencing and in single cells. Intestinal
8 mucosal exposure generated oligoclonal responses which differed from germ-free controls or from the
9 diverse repertoire generated after intravenous systemic exposure. The IgA repertoire, predominantly to cell-
10 surface antigens, did not expand following dose escalation, whereas increased systemic exposure broadened
11 the IgG repertoire to both microbial cytoplasmic and cell-surface antigens. These microbial exposures
12 induced characteristic immunoglobulin heavy chain B cell repertoires mainly at memory and plasma cell
13 stages. Whereas sequential systemic exposure to different taxa diversified the IgG repertoire and facilitated
14 alternate specific responses, sequential mucosal exposure produced limited overlapping repertoires and
15 attrition of initial IgA binding specificities. This shows a contrast between a flexible response to systemic
16 exposure with the need to avoid fatal sepsis, and a restricted response to mucosal exposure reflecting the
17 generic nature of mucosal microbial mutualism.

18 **TEXT**

19 Mammalian immunoglobulins (Ig) are composed of heavy (H) and light (L) chains, each assembled from
20 one of many V_{H/L}, (D_H) and J_{H/L} gene segments during B cell development. The resulting genetic and
21 structural immunoglobulin repertoire diversity and antigen recognition possibilities are further increased by
22 additional nucleotide insertion during recombination, later somatic mutation, or class switch recombination
23 from IgM and/or IgD to IgG, IgE or IgA. Selection and clonal expansion of particular B cells with an
24 appropriate immunoglobulin specificity endows the system to respond to a huge variety of antigens.
25 Comparisons of colonized and germ-free animals show that B cell numbers and immunoglobulin levels
26 (especially IgG and IgA) are considerably amplified by colonization with a microbiota, some of which
27 penetrate mucous membranes to prime systemic secondary lymphoid structures even in healthy hosts.^{4,5} B
28 cell repertoires have so far been shown to be largely unique to each individual animal^{1,2}, although whether
29 this is caused by differences in microbiota composition or the sequence of colonization in each animal is
30 unknown.

31 Using localized time-limited exposures of defined doses of single benign microbial taxa in germ-free
32 animals³, we have addressed how the B cell repertoire is shaped by microbiota exposure at mucous
33 membranes or in systemic lymphoid tissues, and how interactions between different exposure sites or
34 subsequent exposures to different taxa affects the outcome.

35 ***Distinct B cell Ig repertoires to intestinal microbes depending on mucosal or systemic exposure site***

36 We used standardized doses of the live non-replicating *E. coli* strain HA107 to transiently expose germ-free
37 mice to live microbes, either confined within the intestine or via the blood stream. After exposure, all mice
38 rapidly return to germ-free status, owing to HA107 auxotrophy for the essential bacterial amino acids D-
39 alanine and diaminopimelic acid.³ We found distinct antibody repertoires computed on the basis of CDR3
40 heavy chain amino acid identity⁶ from entire IgA, IgG and IgM repertoires, depending on whether the
41 exposure had been mucosal or systemic (Figure 1a-c, Extended data Figure 1a). Clonotype overlap was

42 significantly greater within each exposure condition compared with different conditions (Figures 1a-c right
43 panels) and different exposure conditions segregated in unsupervised tree clustering (Figures 1a-c lower
44 panels). A clear separation according to microbial exposure condition was also found with shared clonotypes
45 computed as sequences encoded by the same V_H and J_H segments, with an identical nucleotide sequence in
46 the CDR3 region ⁷ (Extended Data Figure 1b-g).

47 We used *Clostridium orbiscindens* (DMSZ 8061) as a second transitory colonizing taxon to confirm that the
48 repertoires depend on route of microbial exposure (Figure 1d and Extended Data Figure 1h). Flow
49 cytometric sorting prior to analysis with standardized B cell subset numbers showed that the distinct effects
50 of different microbial exposure routes occurred in the memory and plasma cells (Figure 1e). Although single
51 cell experiments currently only capture a fraction of the clonotype repertoire compared with bulk analysis (in
52 our case $14 \pm 6\%$ $\bar{x} \pm SD$, $n=8$), an MDS plot combining the heavy and light chain information also segregated
53 according to exposure route (Figure 1f). Subsequent analysis considering single cell heavy chain and light
54 chain clonotypes individually showed that the selective effects of microbial exposure route segregate with
55 the Ig heavy chain (Figure 1g).

56 Using bacterial-specific flow cytometry, we verified a preferential isotype class switch to IgG2b after
57 systemic exposure or IgA after mucosal exposure (Extended Data Figure 1i and j) ³. In line with recent
58 reports ⁸⁻¹², we also found that mucosal exposure could generate a small serum IgG response (red symbols
59 Extended Data Figure 1k). Conversely, exclusive systemic exposure generated a specific secretory IgA
60 response in the intestine (blue symbols Extended Data Figure 1l), confirming that both the mucosal and
61 systemic immune systems can be primed by microbial exposure from either route.

62 Alternative approaches are being used by different laboratories to avoid clonal frequency over-estimation
63 due to sequencing errors. We carried out a series of control experiments to confirm that equivalent biological
64 clustering results were obtained with either computational consolidation or use of unique molecular
65 identifier barcodes (Extended Data Figure 2a-c). Although each set of bulk sequencing results in this paper
66 are from samples processed together in a batch, we also verified the technical reproducibility of the same
67 sample processed on different occasions (Extended Data Figure 2d).

68 Different thresholds of Ig priming according to microbial exposure route

69 In our non-replicating transitory exposure system in germ-free mice, test doses can be calibrated without
70 further expansion in vivo. We showed that mucosal doses of 10^6 - 10^8 colony forming units (c.f.u) were
71 needed in order to reshape the mucosal IgH repertoire (Extended Data Figure 3a, e and f) in line with the
72 high doses known to induce specific IgA binding (Extended Data Figure 3b and ³). In contrast, the systemic
73 IgH repertoire was reshaped by as little as 10,000 c.f.u. (Extended Data Figure 3c, g and h). The doses
74 required for detectable humoral responses were generally at least an order of magnitude greater than for
75 repertoire programming (Extended Data Figure 3b and d).

76 Differential B cell targeting of microbial subfractions according to in vivo exposure route

77 To ask why Ig heavy chain clonotype repertoires differed depending on mucosal or systemic microbial
78 exposure, we investigated the targets for bacterial antigen binding according to exposure route. Intestinal
79 IgA bound most effectively to the purified bacterial membrane fraction of *E. coli*, whereas serum IgG bound
80 to both membrane and cytoplasmic fractions (Figure 2a). Ribosomal proteins of *E. coli* dominated the

81 cytoplasmic binding of serum IgG antibodies and were confirmed in a second context by proteomic analysis
82 in SPF mice systemically exposed to *Enterobacter cloacae* (Extended Data Figure 4a-c). Increased exposure
83 of bacterial membranes relative to the cytoplasmic contents in the mesenteric lymph nodes after intestinal
84 treatment was shown by higher lipopolysaccharide/16S ribosome ratios compared with the spleen after
85 systemic treatment (Extended Data Figure 4d). These differences may be caused by the intestinal efficiency
86 of bacterial lipid uptake compared with bacterial cytoplasmic protein contents, whereas systemic exposure
87 would prime equivalent immune responses to membrane and cytoplasmic fractions after opsonization and
88 phagocytosis^{13,14}. Supporting this, B cell clonotype repertoires after systemic (but not mucosal) challenge
89 with ultrasound lysed bacteria overlapped with the repertoires after exposure with intact bacteria (Extended
90 Data Figure 4e and f). Conversely, in the absence of local anatomic processing, the intrinsic antigen-specific
91 and -nonspecific responses to membrane or cytoplasmic bacterial antigens presented directly *in vitro* did not
92 differ depending on mesenteric or splenic B cell origin (Extended Data Figure 4g). We concluded that the
93 different repertoires from mucosal or systemic B cell priming are a consequence of the way in which
94 microbial membrane and cytoplasmic antigens are processed and presented in the different anatomic
95 compartments.

96 *IgA repertoire restriction and IgG repertoire expansion with increased microbial exposure doses*

97 IgA has previously been found to be oligoclonal^{15,16}. We next followed how repertoire expansion or
98 restriction developed according to isotype, exposure route and dose. Whereas IgG diversity generally
99 increased considerably after systemic exposure, no IgA diversity increase in any tissue was found after
100 maximal mucosal exposure (Figure 2b), and both were considerably less than IgM diversity (Extended Data
101 Figure 5a). As the mucosal exposure dose increased, CDR3 clonotype diversity in the IgA heavy chain
102 became more restricted, particularly in the mesenteric lymph nodes (Figure 2c). By comparison, IgG heavy
103 chain diversity in both the spleen and MLN was maintained or further increased with higher levels of
104 systemic exposure (Figure 2c). We also confirmed directly in sorted cells that repertoire diversity is
105 increased after systemic microbial exposure in IgG memory and plasma cells but not after either route of
106 exposure in IgA plasma cells (Figure 2d). Transitory exposure by both the systemic and mucosal routes only
107 generated small numbers of somatic mutations which were not significantly increased by increasing the
108 transitory exposure doses (Extended Data Figure 5b and c). The converse of the breadth of the isotype
109 repertoires is the degree of clonal relatedness, which was higher for IgA than for IgG2b (Extended Data
110 Figure 5d and e). Mucosal and systemic exposure clearly have different physical constraints in terms of the
111 epithelial barrier and scalability of local antigen processing and presentation to B cells. Nevertheless, our
112 experiments show that increased mucosal microbial doses only narrow the IgA repertoire whereas the
113 systemic IgG repertoire is progressively diversified as the exposure dose is increased.

114 To compare directly how immunoglobulin heavy and light chain sequences evolve in different animals
115 during microbial exposure at the different sites, we analysed single cell networks of paired heavy and light
116 chains in naïve and class-switched B cells. As shown in Figures 1g, 2e and f, and Extended Data Figure 6a
117 and b, light chain diversity made only a minor contribution to the networks. IgA immunoglobulins in the
118 mesenteric lymph nodes after intestinal exposure predominantly showed heavy chain connectivity including
119 between germ-free and mucosally-stimulated animals, whereas IgG networks from the spleen of
120 systemically exposed animals had very few germ-free sequences (Figure 2e and f). By contrast, germ-free

121 immunoglobulin sequences were present in our analysis of naïve B cells and intercalated into the networks
122 of both mucosally and systemically exposed animals (Extended Data Figure 6a and b). There was
123 spontaneous activation and class-switch recombination to IgA, even in the mesenteric lymph nodes of germ-
124 free animals, whereas splenic B cells became significantly activated after systemic microbial exposure
125 (Extended Data Figure 6c-f). We concluded that there are clear relationships of class-switched
126 immunoglobulin sequences between different microbe exposed animals in both the mesenteric lymph nodes
127 and the spleen. In diversely colonized animals polyspecific antibodies have been shown to arise from
128 specificities in the germ-free repertoire¹⁶. We now show that the developing IgA repertoire characteristic of
129 mucosal exposure is related to the class-switched Ig sequences present in germ-free animals.

130 Oral sensitization of systemic immunoglobulin responses

131 Since mucosal or systemic microbial exposures generate different B cell repertoire responses with different
132 thresholds, we asked whether exposure at one site could determine the characteristics of a secondary
133 response at the other. The real-world situation is that there are variable degrees of sequential exposure in
134 both mucosal and systemic compartments.

135 Oral feeding of a soluble protein antigen tolerises subsequent B- and T cell responses to systemic exposure
136 with the same antigen¹⁷. In contrast, a sequence of microbial mucosal exposure followed by systemic
137 exposure reduced the threshold for the systemic response by several orders of magnitude compared with
138 intestinal exposure alone (Figure 3a, Extended Data Figure 7a). This effect is T cell dependent as the
139 enhanced systemic response could be abrogated through CD4 T cell depletion at the time of the initial
140 intestinal exposure (Extended Data Figure 7c-f). Although systemic responses were sensitized by prior
141 mucosal exposure to the same microbe, this did not work the other way around, as systemic exposure did not
142 reduce the subsequent high threshold for mucosal IgA responses primed by the mucosal route (Figure 3b,
143 Extended Data Figure 7b).

144 Given that individual mucosal and systemic exposures lead to different B cell repertoires, we asked whether
145 the order of sequential exposure (systemic→mucosal or *vice versa*) makes a difference. This showed that for
146 splenic IgM plasma cells the site of first exposure determined the resulting repertoire even after subsequent
147 exposure at a different site (Figure 3c), *although the priming may be dominated by the site of first exposure*.

148 Functional effects on the resultant repertoire after sequential exposures to different microbes

149 Our final question was how IgA and IgG repertoires build up with successive transitory exposures to
150 different microbes. Mucosal exposure to non-replicating *Salmonella typhimurium* HA218 (engineered from
151 a non-invasive non-virulent parent strain on the same principles as *E. coli* HA107¹⁸) attenuated an
152 established mucosal IgA response to *E. coli* HA107, or *vice versa* with the opposite order (Figure 3d, e and
153 Extended Data Figure 8a). In contrast, the broader systemic IgG response to either microbe given
154 systemically was unrestricted irrespective of exposure order (Figure 3h,i and Extended Data Figure 8b). The
155 CDR3 clonotype repertoires were also biased by the latest mucosal exposure, whereas after sequential
156 systemic exposures the clustering was distinct regardless of exposure order (Figure 3g and k). The clonal
157 relatedness and diversity of IgA showed no significant increase after successive treatments, contrasting with
158 increased IgG clonal diversity and relatedness in the spleen as successive systemic treatments were
159 administered (Figure 3f and j). These results are consistent with greater flexibility of new systemic IgG
160 specificities to accommodate a response to another microbe to avoid systemic sepsis, whereas IgA mucosal

161 protection requires more generic and likely lower affinity responses^{2,16} which adapt sequentially to many
162 different varieties of overlapping antigen exposure^{2,19-21}.

163 In this paper we have shown that the route and order of microbial antigen exposures determine the repertoire
164 and functional outcome for B cell immune responses. In general, the systemic exposure thresholds are lower,
165 yet trigger responses that expand and diversify the B cell repertoire in contrast with mucosal exposure. This
166 is consistent with the IgA repertoire building on an evolutionarily-determined baseline, as some of the
167 clonotypes overlap with immunoglobulin sequences from defined natural antimicrobial specificities
168 (Extended Data Table 1). These different functional demands from B cell immunity offer an explanation for
169 the different characteristics of responses of the B cell system against challenges from the microbiota in
170 different host compartments, the expansion of the same B cell clone in multiple Peyer's patches²² and poor
171 responses to the mucosal route for vaccination where limited hygiene results in an increased burden of
172 environmental microbes and recurrent mucosal infections^{23,24}.

173 **ACKNOWLEDGEMENTS**

174 We would like to thank Mercedes Gomez de Agüero, Tosso Leeb, Pamela Nicholson, Markus Geuking and
175 Daniel Candinas. The Clean Mouse Facility is supported by the Genaxen Foundation, Inselspital and the
176 University of Bern. This work was funded by the Swiss National Science Foundation (SNSF
177 310030B_160262, SNSF 310030_179479) and the European Research Council (H2020 ERC-2016-ADG
178 HHMM_Neonates, Grant Agreement: 742195) to A.J.M. S.C.G.V. was funded by a Marie Curie Intra-
179 European Fellowship (FP7-PEOPLE-2013-IEF Project No. 627206), a long-term fellowship from the
180 European Molecular Biology Organization and the Peter Hans Hofschneider Endowed Professorship by
181 Stiftung Experimentelle Biomedizin. V.G. acknowledges the support of UiO:LifeSciences Convergence
182 Environment Immunolingo and EU H2020 iReceptorplus (#825821). S.H. was funded by SNSF grant
183 169791 and ERC StG 281904. K.D.M. was funded by the ERC StG 281785. M. H. was funded by an ERC
184 CoG (HepatoMetaboPath). J.P.L. was supported by a SystemsX Transition Postdoc Fellowship
185 (TPdF2013/139).

186

187 **AUTHOR CONTRIBUTIONS**

H.L., J.P.L., S.C.G.V. and A.M. conceived the study, interpreted data and wrote the manuscript. H.L. and
S.C.G.V. performed most experiments. J.P.L. and V.G. carried out computational analysis. B.Y., M.A.E.L.,
S.R., M.H. and K.D.M. helped with repertoire experiments. O.S. and S.H. contributed bacterial strains and
culture preparation. C.U., M.Z. and I.D.Y. helped with ex-vivo analyses of bacterial fractions and cellular
responses.

188 **COMPETING INTERESTS**

The authors have no competing interests.

189 **SUPPLEMENTARY INFORMATION**

Summary table containing a) summary of sequenced data in the paper; b) top 100 clonotypes in Extended Data Figure 1e-h; c) top 100 clonotypes in Extended Data Figure 3 a and c; and d) SI Figure 1: gating strategy.

190 **REFERENCES**

- 191 1 Lindner, C. *et al.* Age, microbiota, and T cells shape diverse individual IgA repertoires in the
192 intestine. *J Exp Med* **209**, 365-377, (2012).
- 193 2 Lindner, C. *et al.* Diversification of memory B cells drives the continuous adaptation of secretory
194 antibodies to gut microbiota. *Nat Immunol* **16**, 880-888, (2015).
- 195 3 Hapfelmeier, S. *et al.* Reversible microbial colonization of germ-free mice reveals the dynamics of
196 IgA immune responses. *Science* **328**, 1705-1709, (2010).
- 197 4 Berg, R. D. Bacterial translocation from the gastrointestinal tract. *Adv Exp Med Biol* **473**, 11-30,
198 (1999).
- 199 5 Lockhart, P. B. *et al.* Bacteremia associated with toothbrushing and dental extraction. *Circulation*
200 **117**, 3118-3125, (2008).
- 201 6 Xu, J. L. & Davis, M. M. Diversity in the CDR3 region of V(H) is sufficient for most antibody
202 specificities. *Immunity* **13**, 37-45, (2000).
- 203 7 Soto, C. *et al.* High frequency of shared clonotypes in human B cell receptor repertoires. *Nature*
204 **566**, 398-402, (2019).
- 205 8 Koch, M. A. *et al.* Maternal IgG and IgA Antibodies Dampen Mucosal T Helper Cell Responses in
206 Early Life. *Cell* **165**, 827-841, (2016).
- 207 9 Gomez de Aguero, M. *et al.* The maternal microbiota drives early postnatal innate immune
208 development. *Science* **351**, 1296-1302, (2016).
- 209 10 Zeng, M. Y. *et al.* Gut Microbiota-Induced Immunoglobulin G Controls Systemic Infection by
210 Symbiotic Bacteria and Pathogens. *Immunity* **44**, 647-658, (2016).
- 211 11 Chen, Y. *et al.* Microbial symbionts regulate the primary Ig repertoire. *J Exp Med* **215**, 1397-1415,
212 (2018).
- 213 12 Wilmore, J. R. *et al.* Commensal Microbes Induce Serum IgA Responses that Protect against
214 Polymicrobial Sepsis. *Cell Host Microbe* **23**, 302-311 e303, (2018).
- 215 13 Pepys, M. B. Role of complement in induction of antibody production in vivo. Effect of cobra factor
216 and other C3-reactive agents on thymus-dependent and thymus-independent antibody responses. *J*
217 *Exp Med* **140**, 126-145, (1974).
- 218 14 Sorman, A., Zhang, L., Ding, Z. & Heyman, B. How antibodies use complement to regulate
219 antibody responses. *Mol Immunol* **61**, 79-88, (2014).
- 220 15 Stoel, M. *et al.* Restricted IgA Repertoire in Both B-1 and B-2 Cell-Derived Gut Plasmablasts. *J*
221 *Immunol* **174**, 1046-1054, (2005).
- 222 16 Bunker, J. J. *et al.* Natural polyreactive IgA antibodies coat the intestinal microbiota. *Science* **358**,
223 eaan6619, (2017).
- 224 17 Mowat, A. M., Faria, A. M. & Weiner, H. L. in *Mucosal Immunology* Vol. 1 (eds J. Mestecky *et*
225 *al.*) 487-537 (Elsevier, 2005).
- 226 18 Pfister, S. P. *et al.* Uncoupling of invasive bacterial mucosal immunogenicity from pathogenicity.
227 *Nat Commun* **11**, 1978, (2020).
- 228 19 Boursier, L., Dunn-Walters, D. K. & Spencer, J. Characteristics of IgVH genes used by human
229 intestinal plasma cells from childhood. *Immunology* **97**, 558-564, (1999).
- 230 20 Casola, S. *et al.* B cell receptor signal strength determines B cell fate. *Nat Immunol* **5**, 317-327,
231 (2004).
- 232 21 Dunn-Walters, D. K., Boursier, L. & Spencer, J. Hypermutation, diversity and dissemination of
233 human intestinal lamina propria plasma cells. *Eur J Immunol* **27**, 2959-2964, (1997).
- 234 22 Bergqvist, P. *et al.* Re-utilization of germinal centers in multiple Peyer's patches results in highly
235 synchronized, oligoclonal, and affinity-matured gut IgA responses. *Mucosal Immunol* **6**, 122-135,
236 (2013).
- 237 23 Levine, M. M. Immunogenicity and efficacy of oral vaccines in developing countries: lessons from
238 a live cholera vaccine. *BMC Biol* **8**, 129, (2010).
- 239 24 Valdez, Y., Brown, E. M. & Finlay, B. B. Influence of the microbiota on vaccine effectiveness.
240 *Trends Immunol* **35**, 526-537, (2014).

242 **Figure 1: Antibody repertoires in mucosal and systemic tissues following transitory oral or systemic**
243 **exposure with a commensal microbe**

244 Germ-free mice were either orally or systemically primed three times every other day by intragastric (10^{10}
245 c.f.u.) or intravenous (10^8 c.f.u.) *E. coli* HA107 (a-c, e-g), or *Clostridium orbiscindens* (d), and compared
246 with germ-free controls. Immunoglobulin (Ig) repertoire sequencing at 21 days for IgA (a, d), IgG2b (b), and
247 IgM (c) in ileum, mesenteric lymph nodes (MLN), bone marrow (BM) and spleen (SPL) was performed.
248 Left: MDS plot based on Ig heavy chain CDR3 amino acid sequences of the entire repertoire. Right: Tukey
249 plots of clonal overlap between samples of different priming conditions or the same priming condition
250 (sample comparisons from the same mouse were excluded) are shown with arithmetic mean and whiskers
251 extending to 1.5x interquartile range. Two-sided Wilcoxon rank-sum tests were performed with P_{adj} -values
252 as shown. Lower: Hierarchical clustering. Dendrogram branch lengths show distance between repertoires
253 based on CDR3 amino acid sequence similarity with vertical dotted lines designating principal unbiased
254 separations. (e) IgM, IgA and IgG2b of indicated sorted B cell populations at 21 days. Hierarchical
255 clustering dendrograms from the indicated sorted cell populations, branch length shows the distance between
256 CDR3 amino acid repertoires. (f, g) Single cell VDJ repertoire sequencing analysis. (f) MDS plot of distance
257 between repertoires based on combined Ig heavy and light chain CDR3 amino acid sequences. Grey shading
258 visually indicates GF repertoires. (g) Hierarchical clustering of single cell heavy or light chain Ig repertoires
259 from mesenteric lymph nodes and spleen. Data are representative of nine (a-c), two (e) or three (f, g)
260 independent experiments. All datapoints represent organs from individual mice.

261 **Figure 2: Differences between B cell repertoires following systemic or mucosal exposure**
262 Germ-free mice treated with *E. coli* HA107 at the indicated doses either orally or systemically as in Figure 1.
263 (a) Binding of systemic or intestinal antibodies to *E. coli* membrane versus cytoplasmic fractions evaluated
264 using ELISA ($\bar{x}\pm SD$, n=6, two-sided unpaired t-test). (b) Rarefaction plots of Ig heavy chain sequencing at
265 21 days for IgA and IgG2b in MLN and spleen. (c) Ig heavy chain sequencing at 21 days for IgA in MLN
266 and IgG2b in spleen (n=3 mice for each bacterial exposure group and each defined dose, n = 15 germ-free
267 controls, * p=0.036 MLN IgA both cases, p=0.046 spleen and p=0.036 MLN IgG2b, two-sided Wilcoxon
268 rank-sum test). (d) IgM, IgG2b and IgA heavy chain sequencing of splenic sorted B cell populations at 21
269 days, n=6 for each condition. Tukey plots indicate calculated number of clonotypes per 1000 cells in B cell
270 populations. P=0.003 two-sided Wilcoxon rank-sum test. (e, f) Single cell sequencing analysis. Networks
271 built on combined heavy and light chain CDR3 amino acid sequences each from single spleen IgG- (e) or
272 MLN IgA-expressing (f) B cells (singlets excluded: n=1601 and 670 for E and F respectively), edges show
273 Levenshtein distance =1 or 2. Networks show immunoglobulin sequence relationships within and between
274 different mice in the same experiment, colour-coded according to mouse and treatment. Pie charts (left)
275 indicate the percentage of edge connections that are based on Levenshtein distance 1 on the light chain
276 compared to the heavy chain, or (right) indicate the distribution of edge connections between individual B
277 cells within or between exposure conditions. Tukey plots in c and d are shown with arithmetic mean and
278 whiskers of 1.5x interquartile range. Data are representative of two independent experiments. All
279 datapoints are from individual mice.

280 **Figure 3: Antimicrobial antibody responses following combined mucosal and systemic exposure or**
281 **exposure to two different taxa.**

282 (a, b) Germ-free mice were intestinally (a) or systemically (b) exposed with *E. coli* HA107 on alternate days
283 or remained germ-free throughout. On day 21, all mice were intravenously (a) or intestinally (b) exposed
284 with indicated doses of HA107 (schema Extended Data Figure 7a, b). Flow cytometric analysis of specific
285 bacterial binding of serum IgG2b (a) or intestinal IgA (b) on day 42. (c) Germ-free mice were primed as in a
286 and b. Ig-Seq for IgM of sorted splenic plasma cells. MDS plot of repertoire separation. (d-g) Germ-free
287 mice were either mucosally primed with three doses of *E. coli* HA107 or *Salmonella typhimurium* HA218 or
288 remained germ free. At day 21, half of each group received a second schedule of priming with the opposite
289 taxon, n=3 for each condition. (schema Extended Data Figure 8a). (d, e) Bacterial flow cytometry of *E. coli*
290 HA107-specific (d) or *S. typhimurium* HA218-specific (e) intestinal IgA at d42. (f) Comparisons of mean
291 repertoire diversity and median percentage of expanded clonotypes within the IgA repertoires in the spleen
292 and mesenteric lymph nodes. (g) Hierarchical clustering of full-length IgA heavy chain sequences. (h-
293 k) Experimental design as (d-g) except both reversible taxa given systemically, n=3 for each condition
294 (schema Extended Data Figure 8b). (h, i) Bacterial flow cytometry for serum IgG bacterial binding. (j)
295 Comparisons of mean repertoire diversity and median percentage of expanded clonotypes within the IgG2b
296 repertoires in the spleen and mesenteric lymph nodes. (k) Hierarchical clustering of full length IgG2b heavy
297 chain sequences.

298 (f,j) Unpaired two-tailed t-test was performed on the number of expanded clonotypes: Bars show ranges for
299 each dimension. Data are representative of three (a) or two (b-j) independent experiments. All datapoints
300 are from individual mice.

301

302

303 **Extended Data Figure 1: Mucosal and systemic exposure differentially shape the repertoires of the**
304 **various Ig isotypes**

305 Germ-free mice were either orally or systemically primed three times every other day by intragastric (10^{10}
306 c.f.u.) or intravenous (10^8 c.f.u.) delivery of *E. coli* HA107 (a-g) or *Clostridium orbicindens* (h) and
307 compared with germ-free controls. Immunoglobulin heavy chain repertoire clonotypes at day 21 are defined
308 by V and J segment usage in combination with CDR3 nucleotide sequences, except for panel A where
309 clonotypes are based on CDR3 amino acid sequences as in Figure 1. (a) MDS plot of IgA, IgG2b and IgM
310 showing distinct isotype repertoires (in each case all isotypes were sequenced from each individual sample
311 from at least 3 mice). (b-d) MDS plot from ileum, mesenteric lymph nodes (MLN), bone marrow (BM) or
312 spleen (SPL) of immunoglobulin repertoire sequencing for IgA (b), IgG2b (c) and IgM (d). (e-h) Heat maps
313 showing the 100 most abundant non-unique clonotypes for IgA (e, h), IgG2b (f), IgM (g). Clonotype
314 specifics for each panel are shown in the supplementary information. Samples of ileum, BM, MLN and SPL
315 from each mouse are included. Individual mice are colour-coded on the x-axis of heatmaps. (i, j)
316 Immunoglobulins from intestinal wash of intestinally exposed mice (I) or from serum of systemically
317 exposed mice (j) on day 21 were assessed in bacterial flow cytometry for specific IgM, IgG1, IgG2b, IgG2c,
318 IgG3 or IgA binding to *E. coli* HA107. (k, l) *E. coli* HA107 was incubated with day 21 serum or intestinal
319 wash Ig of the three groups of mice followed by detection of bound murine IgG2b (k) or IgA (l) by flow
320 cytometry. All datapoints are from organs of individual mice.

321 **Extended Data Figure 2: Comparison of computational correction method with unique molecular**
322 **identifiers (UMIs) for PCR artifacts and sequencing reproducibility on different occasions**
323 Germ-free mice were either orally or systemically primed three times every other day by intragastric (10^{10}
324 c.f.u.) or intravenous (10^8 c.f.u.) exposure to *E. coli* HA107 and compared with germ-free controls.
325 Immunoglobulin repertoire sequencing at 21 days for IgA in MLN and IgG2b in spleen was performed in
326 parallel from the same RNA samples with 2 different primers containing different UMIs or primers without
327 UMIs. (a, b) MDS plot of MLN IgA (a) or spleen IgG2b (b) repertoires showing Euclidean distance between
328 points representing the similarity between results whether computational correction (filled symbols) or UMI
329 correction (open and cross symbols for the different UMIs) was used. (c) Heatmap based on CDR3 sequence
330 identity reflecting similarity between UMI-corrected and computational-corrected IgG2b repertoires.
331 (d) Identity matrix based on CDR3 sequences of technical replicates of the same biological sample that had
332 been used on two separate occasions for the entire pipeline of cDNA preparation, IgA amplicon PCR, library
333 preparation and MiSeq sequencing. The distinctions between replicate mice and technical repeats are shown
334 in the diagram.

335 **Extended Data Figure 3: Threshold differences for shaping systemic or mucosal B cell repertoires and**
336 **induction of antibody responses**

337 Reversible *E. coli* HA107 were given to germ-free mice at the indicated doses either orally (a, b, e, f) or
338 systemically (c, d, g, h) as in the legend to Figure 1. (a, c) Ig repertoire analysis at 21 days showing
339 heatmaps of the top 100 non-unique clonotypes for IgA and IgG2b in MLN and spleen based on V, J
340 segment usage combined with CDR3 nucleotide sequences. (b, d) Flow cytometric analysis of *E. coli*-
341 specific Ig binding from intestinal or serum samples from the corresponding mice in A and C respectively.
342 (e-h) Hierarchical clustering of the indicated immunoglobulin repertoires. Dendrogram of samples, branch
343 length shows the distance between repertoires based on CDR3 amino acid sequence similarity of entire B
344 cell repertoires. The dotted lines indicate the principal separations in unsupervised analyses as an
345 independent assessment of thresholds of exposure required for repertoire shaping. Each column within the
346 heatmaps or each dilution series from antibody-binding bacterial flow cytometry are from individual
347 mice, in every case 3 mice were used for every experimental condition studied. The supplementary
348 information contains a table specifying the top 100 clonotypes in each case for panels a and c. Data are
349 representative of two independent experiments

350 **Extended Data Figure 4: Differences in microbial antigen processing and presentation in the mucosal**
351 **and systemic compartments**

352 (a) Reversible *E. coli* HA107 were given to germ-free mice at the indicated doses either orally or
353 systemically as in the legend to Figure 1. Binding of systemic or intestinal antibodies to *E. coli* non-
354 ribosomal versus ribosomal proteins of the cytoplasmic fraction evaluated using ELISA ($\bar{x}\pm$ SD, n=6, two-
355 sided unpaired t-test). (b, c) *Enterobacter cloacae* proteins were either separated by FPLC or subject to
356 ribosomal protein purification, prior to 12% SDS-polyacrylamide gel electrophoresis. Silver stain for total
357 protein (B). Western blot for immunoreactivity against serum IgG raised from specific pathogen-free
358 C57BL/6 mice injected with 10^8 c.f.u. *E. cloacae* 20 days previously (c). Control experiments verified
359 earlier published data²⁵ that unmanipulated control mice showed no immunoreactivity against this dominant
360 intestinal aerobe. Proteomic analysis of extracted bacterial ribosomal proteins confirmed identities as
361 follows: 50SL24, 50SL11, 50SL4, 50SL3, 50SL1, 30SS4, 30SS1. (d) Germ-free mice were either orally (n =
362 6) or systemically (n = 5) exposed once by intragastric (10^{10} c.f.u.) or intravenous (10^8 c.f.u.) delivery of *E.*
363 *coli* HA107. Mesenteric lymph nodes and spleens were analysed 18 hours later for LPS levels and 16S
364 rRNA ($\bar{x}\pm$ SD, two-sided unpaired t-test). (e, f) Indicated doses of intact or ultrasound-lysed *E. coli* HA107
365 were administered either orally (e) or systemically (f) three times to germ-free mice every other day and
366 compared to germ-free controls. Ig heavy chain repertoire analysis at 21 days for IgA in mesenteric lymph
367 nodes (e) or IgG2b in the spleen (f). (g) *In vitro* culture of leukocytes from the mesenteric lymph nodes or
368 spleen of germ-free mice stimulated with either cytoplasmic or membrane fractions of *E. coli* HA107.
369 Activated B cells were sorted on day 5 after stimulation and IgM heavy chain sequencing was carried out.
370 (e-g) In all cases Euclidean distance in MDS plots reflects the distance between indicated repertoires based
371 on CDR3 amino acid sequences of the entire B cell repertoire.
372 (a-d) Data are representative of two independent experiments. (e,f and g) Data are from two single
373 experiments. Each datapoint is from the organ of an individual mouse.

374 **Extended Data Figure 5: Network formation of different isotypes depending on transitory microbial**
375 **treatment and comparison with strong cholera toxin immunogen**

376 Germ-free mice were either orally or systemically primed three times every other day by a range of
377 intragastric (10^2 - 10^{10} c.f.u.) or intravenous (10^2 - 10^8 c.f.u.) doses of *E. coli* HA107, compared with priming
378 by cholera toxin or to germ-free controls. (a) Rarefaction plots of immunoglobulin repertoire sequencing at
379 21 days for IgM or IgG2b (inset: same data as in Figure 2b but different y-axis scale) in MLN and spleen.
380 Colour-coding indicates the route of exposure. (b, c) Median number of mutations per clonotype for IgA in
381 the MLN (b) or IgG2b in splenic B cells (c). Tukey plots in each case are shown with whiskers at 1.5x
382 interquartile range (n=3 for each condition). (d, e) Germ-free mice were either orally or systemically primed
383 three times every other day by intragastric (10^{10} c.f.u.) or intravenous (10^8 c.f.u.) delivery of *E. coli* HA107,
384 or by intragastric (15 μ g) or intravenous (15 μ g) delivery of cholera toxin B (CTB) and compared with
385 germ-free controls. Ig repertoire sequencing was carried out for IgA, IgM and IgG2b at 21 days. (d) Tukey
386 plots with whiskers at 1.5x interquartile range indicate proportions of expanded clonotypes (excluding
387 singletons) within the entire CDR3 amino acid IgA repertoire in ileum, MLN and spleen or within the IgG2b
388 repertoire in MLN and spleen after the indicated exposures (n=3 mice in each bacterial/cholera toxin priming
389 group, n=12 germ-free controls, two-sided Wilcoxon rank-sum test). P_{adj} -values as shown. (e) Radial plot
390 showing median values for mutational levels in MLN, ileum and spleen in individual mice. Peripheral
391 displays of representative network structures of clonotypes showing relatedness with edges representing
392 Levenshtein distance 1 (blue). Singletons are shown in orange. (d,e) All conditions were repeated over 10
393 times, except for cholera toxin i.v. priming which was carried out once and cholera toxin intestinal priming
394 which was carried out twice. All datapoints are from individual mice.

395 **Extended Data Figure 6: Characteristics of naïve B cell repertoires following systemic or mucosal**
396 **exposure and sites of B cell activation**

397 (a, b) Characteristics of naïve single cell B cell repertoires corresponding to class-switched single cell
398 repertoires shown in Figure 2e and f. Germ-free mice were either orally or systemically primed three times
399 every other day by intragastric (10^{10} c.f.u.) or intravenous (10^8 c.f.u.) delivery of *E. coli* HA107 and
400 compared with germ-free controls. Single cell VDJ sequencing analysis on day 21. Network built on
401 combined heavy and light chain CDR3 amino acid sequences each from a single splenic (a) or MLN (b)
402 naïve IgD-expressing B cells, excluding singlets (n=4272 or 5672 for A and B respectively). Edges show
403 Levenshtein distance 1 or 2. Networks show the immunoglobulin sequence relationships within and between
404 different mice in the same experiment, colour-coded according to mouse and treatment. Pie charts (left)
405 indicate the percentage of edge connections that are based on a Levenshtein distance of 1 on the light chain
406 compared to the heavy chain, or (right) indicate the distribution of edge connections between individual B
407 cells within or between exposure conditions.

408 (c-d) Germ-free mice were systemically (i.v.) primed with two doses of 10^8 c.f.u. *E. coli* HA107, 7 days
409 apart, and compared with germ-free controls. Lymphocytes from spleen were isolated 18 h after the i.v.
410 injection, stained with fluorescent-labelled antibodies and analysed by flow cytometry. (c) Overall
411 quantifications ($\bar{x}\pm$ SD, n=11 germ-free and 9 systemic exposure) of live GL-7⁺ CD19⁺ lymphocytes as a
412 proportion of all CD19⁺ lymphocytes from two independent experiments. (d) Lymphocytes from spleen were
413 isolated 3d after the last injection for culture. IgA and IgG2b antibody levels were determined in culture
414 supernatants at 5d by ELISA. Plots show pooled data from two experiments (geometric mean, n=7 germ-free
415 and 8 systemic exposure for both isotypes). (e, f) Germ-free mice were reversibly exposed with 3 gavage
416 doses of 10^{10} c.f.u. *E. coli* HA107 and compared with germ-free controls. (e) Overall quantifications ($\bar{x}\pm$ SD,
417 n=4 for each condition) of live GL-7⁺ Bcl-6⁺ CD19⁺ lymphocytes as a proportion of all CD19⁺ lymphocytes
418 from MLN 24 h after the last gavage ($\bar{x}\pm$ SD). (f) Lymphocytes from MLN were isolated 3d after the last
419 injection for culture. IgA and IgG2b antibody levels were determined at 5d in culture supernatants by
420 ELISA. (geometric means, n=4 for each condition except IgG2b intestinal exposure =3). (c-f) P-values with
421 unpaired t-test are indicated as shown in the figure. All datapoints are from individual mice.

422 **Extended Data Figure 7: CD4 T cells are required for systemic immune memory following intestinal**
423 **exposure to reversible *E. coli* HA107**

424 (a, b) Schematic experimental designs to Figures 3a-c: (a) Germ-free mice were either intestinally exposed
425 with 10^{10} c.f.u. reversible *E. coli* HA107 on alternate days or remained germ-free throughout. On day 21, all
426 mice were reversibly intravenously exposed with 10^3 - 10^7 c.f.u. HA107 as shown. Mice were analysed on
427 day 42. (b) As in a, although the initial reversible exposure was given systemically with subsequent
428 reversible intestinal exposures at different doses. (c) Schematic experimental design. Germ-free mice were
429 either mucosally exposed with 3 doses of 10^{10} c.f.u. *E. coli* HA107 on days 0, 2 and 4 or left germ-free. In
430 both groups, half the mice were treated with anti-CD4 depleting antibody i.p. on day -3, the other half
431 received a control isotype. CD4⁺ T cells were absent (<0.1 % of blood leukocytes) from day 0 until at least
432 day 10, but were shown to have recovered by day 21. On day 21, mice were intravenously primed with 10^7
433 c.f.u. *E. coli* HA107. Control groups included intestinally only exposed mice and untreated germ-free mice.
434 (d) Representative dot plots of flow cytometric analysis of the blood on days 0 and 21 in both the isotype
435 and anti-CD4 antibody treated groups. (e) Bacterial flow cytometry at day 42 analysing specific bacterial
436 surface binding against *E. coli* HA107 from serum IgG2b of the indicated groups. (f) Immunoglobulin
437 repertoire sequencing for IgG2b in the spleen on day 42. Euclidean distance in the MDS plot reflects the
438 distance based on CDR3 amino acid sequences of the entire repertoires. Data (c-f) are representative of
439 two independent experiments. Each dilution series (e) or datapoints (f) are from individual mice.

440

441 **Extended Data Figure 8: Experimental schemes to Figure 3**

442 (a) Schematic experimental design to Figure 3d-g: Germ-free mice were either mucosally primed with three
443 doses of 10^{10} c.f.u. *E. coli* HA107 or reversible *Salmonella typhimurium* HA218 on alternate days or
444 remained germ free. At day 21, half of each group received a second schedule of priming, but with the
445 opposite taxon. Recovery of germ-free status was verified after each stage. (b) Schematic experimental
446 design to Figure 3h-k as in panel (a) although both reversible taxa were given systemically at doses of 10^8
447 c.f.u. as shown.

448 METHODS

449 **Mice**

450 Germ-free C57BL/6 mice (either males or females, 8-16 weeks of age) were bred and maintained in flexible-
451 film isolators at the Clean Mouse Facility, University of Bern, Switzerland. Gender balance was ensured in
452 all experimental groups and germ-free status was routinely monitored by culture-dependent and -
453 independent methods. All mouse experiments were performed in accordance with Swiss Federal regulations
454 approved by the Commission for Animal Experimentation of Kanton Bern. Group sample sizes of ≥ 3 mice
455 were determined from preliminary experiments that indicated sufficient power to discriminate repertoire
456 effects. Computational analysis but not experimental processing was blinded to the treatment of each animal.

457

458 **Bacterial culture**

459 *Escherichia coli* HA107 and non-invasive non-virulent *Salmonella typhimurium* HA218 (UK-1 Δasd , Δahr ,
460 $\Delta dadX$, $\Delta metC::tetRA$, $\Delta ssaV::camR$, $\Delta invC::aphT$) were cultured overnight in LB medium containing
461 100 $\mu\text{g/ml}$ meso-DAP and 400 $\mu\text{g/ml}$ D-alanine at 37°C, shaking at 200 rpm³. A full description of in vivo
462 characteristics of the reversible Salmonella strain will be published separately¹⁸. *Enterobacter cloacae* was
463 cultured in LB medium at 37°C, 200 rpm. *Clostridium orbiscindens* (DSMZ 8061) was cultured in BHI
464 medium with additional hemin and vitamin K at 37°C in a Whitley MG500 anaerobic incubator gassed with
465 10% (v/v) H₂, 10% CO₂, and 80% N₂. Reversible colonisations with *Clostridium orbiscindens* (DSMZ 8061)
466 were confirmed through culture-dependent and -independent methods to return to germ free status after live
467 exposure. To prepare gavage solutions or intravenous injections, bacteria were centrifuged for 10 min at
468 4000 g and washed twice with sterile PBS. The required dose was resuspended in 500 μl of sterile PBS and
469 administered to germ-free mice by oral gavage or injection into the tail vein.

470

471 **Preparation of *E. coli* HA107 lysates and subfractions**

472 Overnight culture of *E. coli* HA107 was harvested, washed with PBS and resuspended at 10¹⁰ c.f.u./ml in
473 PBS. Bacterial cells were disrupted by ultrasound using the Bioruptor system for 15 minutes at 4°C
474 (Diagenode, 30 seconds ON/30 seconds off mode). The lysate was centrifuged at 10,000 g for 10 minutes,
475 diluted and sterilized by 0.2 μm filtration before in vivo treatment or further fractionation. The lysate was
476 fractionated into membrane and cytoplasmic fractions by ultracentrifugation (Optima MAX-TL benchtop
477 ultracentrifuge, Beckman) for 10 min 100,000 g. The cytoplasmic supernatant was collected and the pellet
478 containing membranes was resuspended in PBS. An 18-hour ultracentrifugation at 100,000 g was performed
479 on the cytoplasmic fraction to separate the ribosomal fraction from the non-ribosomal fraction²⁶. Protein
480 concentrations were quantified using the Pierce BCA assay kit (Thermo Fisher Scientific).

481

482 **Systemic and intestinal exposure to live reversible *E. coli* HA107**

483 For systemic exposure, germ-free mice were aseptically transferred to a laminar flow hood. Doses (10²-10⁸
484 c.f.u. as shown) of *E. coli* HA107 were administered into the tail vein. For intestinal exposure, mice received
485 10²-10¹⁰ c.f.u. of *E. coli* HA107 by oral gavage within germ-free isolators³. When multiple doses were
486 administered, mice received 3 doses on alternate days. Mice were analysed 2 weeks after administration of
487 the last exposure dose.

488 **Systemic and intestinal priming of immune responses with *E. coli* HA107 lysate**

489 The preparation of bacterial lysates was performed as described above. Germ-free mice were treated with
490 bacterial lysates (dose equivalent to 10^8 intact bacteria) either systemically or orally on alternate days. Mice
491 were analysed 2 weeks after administration of the last priming dose.

492

493 **Combined intestinal and systemic priming with *E. coli* HA107**

494 Germ-free C57BL/6 mice were divided into two groups. In the first scenario, a group of mice was treated
495 with three doses of 10^{10} c.f.u. of HA107 orally on days 0, 2 and 4, whilst the other group were unprimed
496 controls. Both groups of mice (intestinally primed with 3 doses of 10^{10} c.f.u. of *E. coli* HA107 and control
497 mice) received an i.v. injection of $10^3 - 10^7$ c.f.u. (as shown) of *E. coli* HA107 on day 21.

498 In the second converse scenario, a group of mice was treated three times with 10^8 c.f.u. of HA107
499 systemically on days 0, 2 and 4 while the other group were unprimed controls. Both groups of mice
500 subsequently received 3 intragastric doses of $10^7 - 10^9$ c.f.u. (as shown) of *E. coli* HA107 on days 21, 23 and
501 25. All mice from both scenarios were analysed on day 42.

502

503 **Combined priming with *E. coli* HA107 and *S. typhimurium* HA218**

504 For mucosal priming, germ-free mice received 10^{10} c.f.u. of *E. coli* HA107 by gavage on days 0, 2 and 4 or
505 were unprimed controls. Subsequently half the mice in both groups received 3 doses of 10^{10} c.f.u.
506 *S. typhimurium* HA218 on days 21, 23 and 25 by gavage, while the other half received no further priming.
507 Within the same experiment further groups received the opposite treatment sequence of *S. typhimurium*
508 HA218 → *E. coli* HA107. Systemic priming was carried out using groups of germ-free mice with the above
509 schedule in both treatment orders, except that 3 doses of 10^8 c.f.u. of *E. coli* HA107 or *S. typhimurium*
510 HA218 by intravenous injection were used instead of the intestinal treatments for mucosal priming.
511 Recovery of germ-free status was verified at each stage. All mice were analysed on day 42.

512

513 **Priming with cholera toxin subunit B**

514 Germ-free mice each received 3 doses of intragastric (15 μ g) or intravenous (15 μ g) cholera toxin B (CTB)
515 on alternate days and were analyzed 3 weeks after the last priming dose. For intragastric delivery, CTB was
516 dissolved in 0.1M sodium bicarbonate (pH 9), systemic delivery was in PBS.

517

518 **Bacterial FACS**

519 Bacterial FACS was performed as described previously³, with the following refinements. *E. coli* HA107
520 was incubated with serum or intestinal washes with starting dilutions at 1/10 for serum, or undiluted for
521 intestinal washes: in each sample the concentrations of different immunoglobulin isotypes had been
522 measured separately by ELISA as detailed below. After incubation and washing to remove unbound
523 antibodies, the samples were incubated further at 4°C for 2 hours either with secondary anti-murine IgA-
524 FITC (BD Biosciences C10-3) or anti-murine IgG2b-FITC (BD Biosciences R12-3). Bacteria were acquired
525 on a BD FACSAarray using FSC and SSC parameters in logarithmic mode. The FACS data were analysed
526 using FlowJo software (TreeStar, Inc.), and the levels of bacteria-specific antibodies present in the samples
527 were expressed as the geometric mean against the absolute Ig concentration in the sample.

528

529 **ELISA**

530 Immunoglobulin-specific ELISAs were performed as described²⁷ using goat anti-mouse IgA, IgM, IgG1,
531 IgG2b, IgG2c, IgG3 coating antibodies from SouthernBiotech. Antibody standards were purified mouse
532 myeloma Ig of the required isotype with peroxidase-coupled secondary antibodies as previously detailed.
533 The same protocol was used for antigen-specific ELISA except that ELISA plates were first coated
534 overnight with 10 µg/ml of HA107 membrane, cytoplasmic, ribosomal or non-ribosomal fractions.

535

536 **Immunoblotting**

537 Bacterial (*E. cloacae*) cytoplasmic proteins (10 µg/ml) were loaded to 12% SDS-PAGE and electrophoresed
538 for 45 minutes at 90V; subsequently they were either stained directly for proteins or transferred to a
539 nitrocellulose membrane. After blocking with 3% BSA, the membrane was incubated with i.v. primed
540 mouse serum diluted at 1:30 in PBS for 1hr at room temperature. Peroxidase-conjugated goat anti-mouse
541 IgG catalysis of 3, 3'-diaminobenzidine was used to detect bound IgG²⁵.

542

543 **LPS versus 16S rRNA measurements**

544 Germ-free mice were treated either systemically with 10⁸ c.f.u. of *E. coli* HA107 or mucosally with 10¹⁰
545 c.f.u. of *E. coli* HA107. Mice were dissected 18 hours later. Spleen and MLN were collected and
546 disaggregated on baked 40 µm-metal cell strainers using PBS. Samples were then split into two portions for
547 either LPS or 16S rRNA estimation.

548 *LPS measurements*

549 Samples were centrifuged (350 g 5 mins) to remove intact cells. Supernatants were heated at 70°C for 30
550 mins and cleared by centrifugation at 10,000 g. LPS was quantified using the EndoZyme® II Recombinant
551 Factor C Endotoxin Detection Assay (Hyglos GmbH, BioMérieux #890030) according to the manufacturer's
552 instructions, using 10-fold dilutions to circumvent interference. After incubation at 37°C for 90 minutes
553 fluorescence was measured at an excitation of 380 nm and an emission of 445 nm (Infinite Pro 200, Tecan).
554 End point fluorescent measurements with blank corrections and standards from 0.005 - 5 EU/ml were used.
555 Standard curve generation and regression analysis performed in Graphpad prism were used to estimate LPS
556 concentrations in samples, with extrapolation of the standard curve based on the regression parameters.
557 Samples and standards were measured in duplicate.

558 *16S measurements*

559 Total RNA was extracted from samples using the DNA-RNA all prep kit (Qiagen), and real-time PCR was
560 performed on synthesized cDNA using forward (5'-ATG CGT AGA GAT CTG GAG G-3') and reverse
561 primers (5'-CAA CCT CCA AGT CGA CAT C-3') for 16S ribosomal gene amplification.

562

563 **Lymphocyte isolation**

564 To isolate lymphocytes from spleens, lymph nodes and Peyer's patches, tissues were cut into small pieces
565 and digested in IMDM (2 % FCS) containing collagenase type IA (1 mg/ml, Sigma) and DNase I (10 U/ml,
566 Roche) at 37°C for 30 min. Cellular suspensions were passed through a cell strainer (40 µm) and washed
567 with IMDM (2 % FCS, 2mM EDTA). Erythrocytes in splenic suspensions were lysed using 0.84 % NH₄Cl
568 for 2 min at room temperature. Cells were finally resuspended in FACS buffer and counted in a Neubauer
569 chamber.

570

571 **Flow cytometry**

572 After isolation, cells were washed once with PBS before staining with fixable viability dye diluted in PBS
573 (eBioscience) for 30 min on ice. Single cell suspensions were sequentially incubated with primary/biotin-
574 and fluorescence-coupled antibodies diluted in FACS buffer. The following mouse-specific conjugated
575 antibodies were used: B220-FITC (RA3-6B2, Biolegend), Bcl-6-AlexaFluor647 (K112-91, BD
576 Biosciences), CD3-BV785 (17A2, Biolegend), CD4-PE (RM4-5, Biolegend), CD11b-PEcy7 (M1/70,
577 Biolegend), CD19-AF700 (6D5, Biolegend), CD21-FITC (7E9, Biolegend), CD22-FITC (OX-97,
578 Biolegend), CD23-PerCPcy5.5 (B3B4, Biolegend), CD25-PerCP-cy5.5 (PC61, Biolegend), CD43-FITC
579 (1B11, Biolegend), CD80-PerCPcy5.5 (16-10A1, Biolegend), CD86-BV421 (GL-1, biolegend), CD93-
580 PEcy7 (AA4.1, Biolegend), CD138-PE (281-2, Biolegend), CD273-APC (TY25, Biolegend), CXCR5-biotin
581 (2G8, BD Biosciences), IgA-FITC (C10-3, BD Biosciences), IgG2b-FITC (R12-3, BD Biosciences), IgM-
582 PEcy7 (RMM-1, Biolegend), Ly-77-BV421 (GL-7, BD Biosciences), PD-1-PE (RMP1-30, Biolegend).
583 Streptavidin-APC (BD Biosciences) was used together with biotin-coupled antibodies. Data were acquired
584 on an LSRFortessa (BD Biosciences) and analysed using FlowJo software (Tree Star Inc.). In all
585 experiments, FSC-H versus FSC-A was used to gate singlets, and to exclude dead cells using the
586 fluorescence-coupled fixable viability dye (eBioscience). B-lineage subsets were stained for flow cytometry
587 cell sorting as: pre B cells from bone marrow (live/dead⁻ CD3⁻ CD19⁺ CD138⁻ IgM⁻ CD25⁺), plasma cells
588 from bone marrow (live/dead⁻ CD3⁻ CD138⁺ CD19⁻ CD22⁻), transitional B cells from spleen (live/dead⁻
589 CD3⁻ CD19⁺ CD138⁻ GL7⁻ CD93⁺), splenic IgM⁺ plasma cells (live/dead⁻ CD3⁻ CD19⁻ CD138⁺ IgM⁺),
590 splenic IgG2b⁺ plasma cells (live/dead⁻ CD3⁻ CD19⁻ GL7⁻ CD138⁺ IgG2b⁺), follicular splenic B cells
591 (live/dead⁻ CD3⁻ CD19⁺ CD93⁻ CD138⁻ CD23^{hi} CD21^{lo}), splenic marginal zone B cells (live/dead⁻ CD3⁻
592 CD19⁺ CD93⁻ CD138⁻ CD23^{lo} CD21^{hi}), splenic IgM⁺ memory cells (live/dead⁻ CD3⁻ CD19⁺ CD138⁻ CD80⁺
593 CD273⁺ IgM⁺)²⁸, splenic IgG2b⁺ memory cells (live/dead⁻ CD3⁻ CD19⁺ GL7⁻ CD138⁻ IgG2b⁺), peritoneal
594 B2 cells (live/dead⁻ CD3⁻ CD19⁺ CD23⁺ CD43⁻), peritoneal B1a cells (live/dead⁻ CD3⁻ CD19⁺ CD23⁻ CD43⁺
595 B220^{lo} IgM^{hi}), peritoneal B1b cells (live/dead⁻ CD3⁻ CD19⁺ CD23⁻ CD11b⁺ B220^{hi} IgM^{lo}), splenic/MLN
596 IgA⁺ plasma cells (live/dead⁻ CD3⁻ CD19⁻ GL7⁻ CD138⁺ IgA⁺).

597

598 ***In vitro* primary cell culture**

599 Primary cells were isolated from spleen, PP and MLN from germ-free or *E. coli* HA107 conditioned mice.
600 Tissues were disaggregated through 40 µm cell strainers and flushed with 10 ml IMDM+GlutaMax (GIBCO)
601 supplemented with 10% FCS (Invitrogen). Cell suspensions were centrifuged (350 g, 5 min, 4°C) and
602 erythrocyte lysis from splenic samples was performed as described above.

603 For the estimation of IgA and IgG2b production by B cells, cells were centrifuged again and resuspended in
604 complete IMDM medium IMDM+GlutaMAX (GIBCO), supplemented with 10% FCS (Invitrogen), 10,000
605 µg/ml streptomycin (GIBCO), 10,000 U/ml penicillin (GIBCO), 50 µM 2-mercaptoethanol (Merck). The cell
606 suspensions were seeded at a density of 10⁶ cells/ml in 200 µl of complete IMDM medium per well in 96-
607 well round-bottom tissue culture plates. The cell cultures were incubated at 37°C, 5% CO₂. Viability of the
608 cultured cells was controlled daily microscopically. Supernatants were collected after 5 days and antibody
609 concentrations were determined using ELISA as described above.

610 For the assessment of repertoire reprogramming to antigen exposure, an aliquot of cells was collected and

611 CD86⁺ CD138⁺ antigen-experienced plasma cells were sorted and used as pre-treatment controls. Remaining
612 cells were seeded at a density of 10⁶ cells/ml in RPMI 1640 medium supplemented with FCS, streptomycin,
613 penicillin, and β-mercaptoethanol as above with the addition of 10 ng/ml recombinant IL4 (Peprotech) in a
614 48-well flat-bottomed plate. *E. coli* cytoplasmic and membrane fractions were added at 5 μg/ml (protein
615 equivalent) to culture wells. The culture conditions were as detailed above. On day 6, cells were harvested,
616 and CD86⁺ CD138⁺ plasma cells were FACS-sorted for repertoire analysis.

617

618 **CD4 T cell depletion**

619 Germ-free mice were injected intraperitoneally either with 250 μg of anti-CD4 antibody (clone GK5.1,
620 Bioexcel) or an isotype control (clone LTF-2, Bioexcel) diluted in 250 μl of PBS on day -3 before intestinal
621 exposure with 3 x 10¹⁰ c.f.u. *E. coli* HA107 on days 0, 2 and 4. T cell depletion and recovery were confirmed
622 by flow cytometry on blood samples taken on days 0 and 21 respectively. All mice received a single
623 intravenous dose of 10⁷ c.f.u. *E. coli* HA107 on day 21. Mice were analysed on day 42.

624

625 **Immunoglobulin repertoire sequencing bulk**

626 Tissues were removed and snap-frozen in Trizol reagent using liquid nitrogen. Thawed tissues were
627 immediately homogenized (Retsch bead-beater) in 1 ml of Trizol reagent (Life Technologies). Chloroform
628 (200 μl) was added, samples were mixed, and centrifuged (12,000 g, 15 min, 4°C). The upper phase was
629 collected, and RNA was precipitated with ice-cold isopropanol by centrifugation (12,000 g, 10 min, 4°C).
630 The RNA pellet was washed with 75% (v/v) ethanol, dried and resuspended in RNase-free water. RNA
631 concentrations and purity were analysed using a Nanodrop2000 (Thermo Scientific).

632 For IgA, cDNA synthesis was performed by mixing 700 ng of RNA, 1 μl of 2 μM gene specific primer
633 mix¹, 1 μl of 10 mM of dATP, dCTP, dGTP and dTTP (Invitrogen), with dH₂O to a total volume of 13 μl.
634 For IgM and IgG2b heavy chains and light chains, oligo(dT) primers were used for cDNA synthesis.
635 Samples were then heated to 65°C for 5 min, after which they were put on ice for a minimum of 1min. Tubes
636 were shortly centrifuged to collect contents, and in a second reaction step, 4 μl 5X first strand buffer
637 (Invitrogen), 1 μl 0.1 M DTT (Invitrogen), 1 μl RNaseOUT (Invitrogen) and 1μl Superscript III RT enzyme
638 (Invitrogen) were added to the reaction, mixed and incubated at 55°C for 50 min. The reaction was
639 terminated by heat inactivation at 70°C for 15 min followed by cooling at 4°C. Samples were stored at -20°C
640 until further processing.

641 Amplicon PCR for IgA, IgM or IgG2b heavy chains and kappa or lambda light chains was performed by
642 mixing 5 μl of 10X PlatinumTaq PCR buffer (Qiagen), 1 μl of 10 mM mixed dNTPs, 0.2 μl of PlatinumTaq
643 DNA Polymerase (Qiagen), 1.5 μl of 50 mM MgCl₂, 1 μl of each 100 μM forward primer mix and reverse
644 primers (sequences see below according to chain and isotype), 5 μl template cDNA, in a total volume of
645 50 μl. The forward primers consisted of a degenerative mix of 19 different primers binding into FR1 as
646 previously described^{29,30}. Reverse primers were complementary to the constant region of each isotype
647 (sequences see below).

648 PCR products were loaded onto a 1.5% (w/v) agarose gel and purified with the QIAquick Gel Extraction kit
649 (QIAGEN) according to the manufacturer's instructions. The purified DNA was tested for quality and
650 quantity using a 2100 Bioanalyzer (Agilent) and Qbit (Thermofisher). A second PCR was performed to
651 attach sample indices and sequencing adapters using the Nextera® XT Index Kit (Illumina). Subsequent

652 sample sizes and quality were tested with a Fragment Analyzer™ (Advanced Analytical), normalized and
 653 libraries were pooled for sequencing on the MiSeq Illumina sequencer in the paired 250bp mode, or the
 654 300bp mode for experiments containing UMIs.

655

656 **Primer sequences**

IgH Forward Mix	Illumina Adapter sequence read 1 + Diversity region + VH 5' specific Region
IgH-UAd-fw1	TCGTCGGCAGCGTCAGATGTGTATAAGAGACAGNNNNGAKGTRMAGCTTCAGGAGTC
IgH-UAd-fw2	TCGTCGGCAGCGTCAGATGTGTATAAGAGACAGNNNNGAGGTBCAGCTBCAGCAGTC
IgH-UAd-fw3	TCGTCGGCAGCGTCAGATGTGTATAAGAGACAGNNNNCAGGTGCAGCTGAAGSASTC
IgH-UAd-fw4	TCGTCGGCAGCGTCAGATGTGTATAAGAGACAGNNNNGAGGTCCARCTGCAACARTC
IgH-UAd-fw5	TCGTCGGCAGCGTCAGATGTGTATAAGAGACAGNNNNCAGGTTCAGCTBCAGCARTC
IgH-UAd-fw6	TCGTCGGCAGCGTCAGATGTGTATAAGAGACAGNNNNCAGGTTCARCTGACGACGTC
IgH-UAd-fw7	TCGTCGGCAGCGTCAGATGTGTATAAGAGACAGNNNNCAGGTCCACGTGAAGCAGTC
IgH-UAd-fw8	TCGTCGGCAGCGTCAGATGTGTATAAGAGACAGNNNNGAGGTGAASSTGGTGAATC
IgH-UAd-fw9	TCGTCGGCAGCGTCAGATGTGTATAAGAGACAGNNNNGAVGTGAWGYTGGTGGAGTC
IgH-UAd-fw10	TCGTCGGCAGCGTCAGATGTGTATAAGAGACAGNNNNGAGGTGCAGSKGGTGGAGTC
IgH-UAd-fw11	TCGTCGGCAGCGTCAGATGTGTATAAGAGACAGNNNNGAKGTGCAMCTGGTGGAGTC
IgH-UAd-fw12	TCGTCGGCAGCGTCAGATGTGTATAAGAGACAGNNNNGAGGTGAAGCTGATGGARTC
IgH-UAd-fw13	TCGTCGGCAGCGTCAGATGTGTATAAGAGACAGNNNNGAGGTGCARCTTGTGGAGTC
IgH-UAd-fw14	TCGTCGGCAGCGTCAGATGTGTATAAGAGACAGNNNNGARGTRAAGCTTCTCGAGTC
IgH-UAd-fw15	TCGTCGGCAGCGTCAGATGTGTATAAGAGACAGNNNNGAAGTGAARSTTGAGGAGTC
IgH-UAd-fw16	TCGTCGGCAGCGTCAGATGTGTATAAGAGACAGNNNNCAGGTACTCTRAAAGWGTSTG
IgH-UAd-fw17	TCGTCGGCAGCGTCAGATGTGTATAAGAGACAGNNNNCAGGTCCAACVTCAGCARCC
IgH-UAd-fw18	TCGTCGGCAGCGTCAGATGTGTATAAGAGACAGNNNNGATGTGAACVTCGAAGTGTCT
IgH-UAd-fw19	TCGTCGGCAGCGTCAGATGTGTATAAGAGACAGNNNNGAGGTGAAGTCACTCGAGTC
IgH Reverse (isotype specific)	Illumina Adapter sequence read 2 + diversity region + Ig constant region specific
IgA-const-rev	GTCTCGTGGGCTCGGAGATGTGTATAAGAGACAGNNNNGAGCTCGTGGGAGTGCAGTC
IgM-const-rev	GTCTCGTGGGCTCGGAGATGTGTATAAGAGACAGNNNNGAGACGAGGGGAAGACATT
IgG2b-const-rev	GTCTCGTGGGCTCGGAGATGTGTATAAGAGACAGNNNNTTGTATCTCCACACCCAGGG

IgH Forward UMI	Illumina Adapter sequence read 2 + Diversity region + VH 5' specific Region
IgH-UAd-fw1_UMI	GTCTCGTGGGCTCGGAGATGTGTATAAGAGACAGNNNNGAKGTRMAGCTTCAGGAGTC
IgH-UAd-fw2_UMI	GTCTCGTGGGCTCGGAGATGTGTATAAGAGACAGNNNNGAGGTBCAGCTBCAGCAGTC
IgH-UAd-fw3_UMI	GTCTCGTGGGCTCGGAGATGTGTATAAGAGACAGNNNNCAGGTGCAGCTGAAGSASTC
IgH-UAd-fw4_UMI	GTCTCGTGGGCTCGGAGATGTGTATAAGAGACAGNNNNGAGGTCCARCTGCAACARTC
IgH-UAd-fw5_UMI	GTCTCGTGGGCTCGGAGATGTGTATAAGAGACAGNNNNCAGGTTCAGCTBCAGCARTC
IgH-UAd-fw6_UMI	GTCTCGTGGGCTCGGAGATGTGTATAAGAGACAGNNNNCAGGTTCARCTGACGACGTC
IgH-UAd-fw7_UMI	GTCTCGTGGGCTCGGAGATGTGTATAAGAGACAGNNNNCAGGTCCACGTGAAGCAGTC
IgH-UAd-fw8_UMI	GTCTCGTGGGCTCGGAGATGTGTATAAGAGACAGNNNNGAGGTGAASSTGGTGAATC
IgH-UAd-fw9_UMI	GTCTCGTGGGCTCGGAGATGTGTATAAGAGACAGNNNNGAVGTGAWGYTGGTGGAGTC
IgH-UAd-fw10_UMI	GTCTCGTGGGCTCGGAGATGTGTATAAGAGACAGNNNNGAGGTGCAGSKGGTGGAGTC
IgH-UAd-fw11_UMI	GTCTCGTGGGCTCGGAGATGTGTATAAGAGACAGNNNNGAKGTGCAMCTGGTGGAGTC
IgH-UAd-fw12_UMI	GTCTCGTGGGCTCGGAGATGTGTATAAGAGACAGNNNNGAGGTGAAGCTGATGGARTC
IgH-UAd-fw13_UMI	GTCTCGTGGGCTCGGAGATGTGTATAAGAGACAGNNNNGAGGTGCARCTTGTGGAGTC
IgH-UAd-fw14_UMI	GTCTCGTGGGCTCGGAGATGTGTATAAGAGACAGNNNNGARGTRAAGCTTCTCGAGTC
IgH-UAd-fw15_UMI	GTCTCGTGGGCTCGGAGATGTGTATAAGAGACAGNNNNGAAGTGAARSTTGAGGAGTC
IgH-UAd-fw16_UMI	GTCTCGTGGGCTCGGAGATGTGTATAAGAGACAGNNNNCAGGTACTCTRAAAGWGTSTG
IgH-UAd-fw17_UMI	GTCTCGTGGGCTCGGAGATGTGTATAAGAGACAGNNNNCAGGTCCAACVTCAGCARCC
IgH-UAd-fw18_UMI	GTCTCGTGGGCTCGGAGATGTGTATAAGAGACAGNNNNGATGTGAACVTCGAAGTGTCT
IgH-UAd-fw19_UMI	GTCTCGTGGGCTCGGAGATGTGTATAAGAGACAGNNNNGAGGTGAAGTCACTCGAGTC
Reverse UMI_1	Illumina Adapter sequence read 1 + UMI_1 + IgA constant region specific
IgG2b-const-rev_UMI_1	TCGTCGGCAGCGTCAGATGTGTATAAGAGACAGNNNNNNNNNNNNNNNNTTGTATCTCCACACCCAGGG
IgA-const-rev_UMI_1	TCGTCGGCAGCGTCAGATGTGTATAAGAGACAGNNNNNNNNNNNNNNNGAGCTCGTGGG AGTGTCTAGTC
Reverse UMI_2	Illumina Adapter sequence read 1 + UMI_2 + IgA constant region specific
IgG2b-const-rev_UMI_2	TCGTCGGCAGCGTCAGATGTGTATAAGAGACAGHHHHHHACAHHHHHHACAHHHHHHNTTGTATCTCCACACCCAGGG
IgA-const-rev_UMI_2	TCGTCGGCAGCGTCAGATGTGTATAAGAGACAGHHHHHHACAHHHHHHACAHHHHHHNGAGCTCGTGGGAGTGTCTAGTC

IgL Forward Mix	Illumina Adapter sequence read 1 + Diversity region + VH 5' specific Region
IgL_nonfw1	TCGTCGGCAGCGTCAGATGTGTATAAGAGACAGNNNNAYATCCAGCTGACTCAGCC
IgL_nonfw2	TCGTCGGCAGCGTCAGATGTGTATAAGAGACAGNNNNAYATTGTCTCWCACAGTC
IgL_nonfw3	TCGTCGGCAGCGTCAGATGTGTATAAGAGACAGNNNNAYATTGTCTCWCACAGTC
IgL_nonfw4	TCGTCGGCAGCGTCAGATGTGTATAAGAGACAGNNNNAYATTGTGYTRACACAGTC
IgL_nonfw5	TCGTCGGCAGCGTCAGATGTGTATAAGAGACAGNNNNAYATTGTRATGACMCAGTC

IgL_nonfw6	TCGTCGGCAGCGTCAGATGTGTATAAGAGACAGNNNNAYATTMAGATRAMCCAGTC
IgL_nonfw7	TCGTCGGCAGCGTCAGATGTGTATAAGAGACAGNNNNAYATTCAGATGAYDCAGTC
IgL_nonfw8	TCGTCGGCAGCGTCAGATGTGTATAAGAGACAGNNNNAYATYCAGATGACACAGAC
IgL_nonfw9	TCGTCGGCAGCGTCAGATGTGTATAAGAGACAGNNNNAYATTGTTCTCAWCCAGTC
IgL_nonfw10	TCGTCGGCAGCGTCAGATGTGTATAAGAGACAGNNNNAYATTGWGCTSACCCAATC
IgL_nonfw11	TCGTCGGCAGCGTCAGATGTGTATAAGAGACAGNNNNAYATTSTRATGACCCARTC
IgL_nonfw12	TCGTCGGCAGCGTCAGATGTGTATAAGAGACAGNNNNAYRTTKGTATGACCCARAC
IgL_nonfw13	TCGTCGGCAGCGTCAGATGTGTATAAGAGACAGNNNNAYATTGTGATGBCBAGKC
IgL_nonfw14	TCGTCGGCAGCGTCAGATGTGTATAAGAGACAGNNNNAYATTGTGATAACYCAGGA
IgL_nonfw15	TCGTCGGCAGCGTCAGATGTGTATAAGAGACAGNNNNAYATTGTGATGACCCAGWT
IgL_nonfw16	TCGTCGGCAGCGTCAGATGTGTATAAGAGACAGNNNNAYATTGTGATGACACAACC
IgL_nonfw17	TCGTCGGCAGCGTCAGATGTGTATAAGAGACAGNNNNAYATTTTG CTGACTCAGTC
IgL_nonfw18	TCGTCGGCAGCGTCAGATGTGTATAAGAGACAGNNNNARGCTGTTGTGACTCAGGAATC
IgL Reverse	Illumina Adapter sequence read 2 + diversity region + IgL constant region specific
IgL_rev1	GTCTCGTGGGCTCGGAGATGTGTATAAGAGACAGNNNNACGTTTGATTTCCAGCTTGG
IgL_rev2	GTCTCGTGGGCTCGGAGATGTGTATAAGAGACAGNNNNACGTTTATTTCCAGCTTGG
IgL_rev3	GTCTCGTGGGCTCGGAGATGTGTATAAGAGACAGNNNNACGTTTATTTCCAACITTTG
IgL_rev4	GTCTCGTGGGCTCGGAGATGTGTATAAGAGACAGNNNNACGTTTCAGCTCCAGCTT GG
IgL_rev5	GTCTCGTGGGCTCGGAGATGTGTATAAGAGACAGNNNNACCTAGGACAGTCAGTTTGG
IgL_rev6	GTCTCGTGGGCTCGGAGATGTGTATAAGAGACAGNNNNACCTAGGACAGTGACCTTGG

657 Repertoire sequencing and pre-processing

658 Antibody variable heavy chain (VH) libraries were prepared as previously described³¹ and sequenced on the
659 Illumina MiSeq platform (2x250 cycles, paired-end) with 10% PhiX control library. Mean base call quality
660 of all samples was in the range of Phred score 30. The resulting FASTQ files were pre-processed (VDJ
661 alignment, clonotyping) using the MiXCR software package v2.1.12 (clonotype formation by CDR3 amino
662 acid region annotated using C57BL/6J germline gene data³² (available at <http://mixcr.milaboratory.com/> and
663 <https://github.com/milaboratory/mixcr/>).

664 MIXCR considers sequence quality and corrects PCR and sequencing errors in the alignment step to the
665 reference V, D, J germline segments. The error correction is done by assembling the clonotypes with a
666 heuristic multi-layer clustering which briefly can be summarized as follows : the algorithm consists of two
667 steps: (A) a K-mer chaining algorithm is used, then in order to find the optimal reference sequence a
668 heuristic search is performed to maximize a scoring function which takes into account variations (deletions,
669 insertions, mutations) in the sequence reads. (B) Subsequently, multiple candidate alignments are built and a
670 classical alignment score (scoring matrix and penalties for indels) is calculated. Reads are filtered based on
671 these values. Then clonotypes are assembled and those presenting errors are further removed by clustering
672 similar sequences based on a defined similarity threshold (clonotyping). Finally, MIXCR rescues low-
673 quality reads in a later step by mapping them to previously assembled high-quality clonotypes to preserve
674 maximal quantitative information. Singletons (supported by only a single read) were excluded from
675 clonotype output^{29,32} as previously described³³.

676 For all analyses, except where nucleotide analysis combined with V and J segment information is specified,
677 clones were defined by 100% amino acid sequence identity of CDR3 regions. CDR3 regions were defined
678 by MiXCR according to the nomenclature of the Immunogenetics database (IMGT)³⁴.

679

680 Clonal analysis and quantification of repertoire convergence

681 MIXCR output files were further processed in VDJtools post-analysis framework³⁵ (available at
682 <https://github.com/mikessh/vdjtools>) to further analyse clonotype diversity, V gene usage and sample
683 clustering based on CDR3 abundance. Further filtering was applied in order to keep only in-frame,
684 productive sequences. Basic statistic segment usage was calculated, and weighted variable usage profiles

685 were hierarchically clustered and visualized as heatmaps. Repertoire overlap was measured by calculating
686 the geometric mean of relative overlap frequencies between variable segment usage profiles or CDR3 amino
687 acid sequence usage. The relative overlap similarity was represented as hierarchical clustering or multi-
688 dimensional scaling (MDS) plots. Heatmaps following the top100 clonotypes (ranked by abundance) present
689 in at least 2 samples were generated based on an all-vs-all intersection between chosen samples with settings
690 = “strict”, meaning intersections had to contain the identical nucleotide sequence (CD3nt sequence + V gene
691 + J gene). The corresponding CDR3 amino acid sequences are provided in the supplementary information
692 table respective to each heatmap found in the figures.

693

694 **Technical replicate sequencing and UMI pre-processing**

695 Technical reproducibility as previously described^{29,31} was tested on cDNA derived from 9 C57BL/6 mice.
696 cDNA was split into three portions and library preparation was performed in parallel with different Illumina
697 indices as described above. Replicate samples were sequenced with the same sequencing depth. cDNA was
698 amplified using primers with the alternative primer design approaches of 15 nucleotide unique molecular
699 identifiers (UMI_1)³⁶ or with UMI with fixed positions preventing secondary structures (UMI_2)³⁷ by PCR
700 in a multiplex reaction using primer sets as mentioned above. Raw reads were demultiplexed and exported
701 without the sample barcodes or Illumina clustering adapters. Pre-processing of the raw demultiplexed reads
702 was carried out using pRESTO³⁸. Reads with a mean Phred quality score below 20 were removed, then
703 those without valid forward (V-region) and reverse (isotype/constant region) primer sequence matches were
704 removed (match error rate of 0.2). The forward primer regions were masked (with Ns) and the reverse
705 primer regions were deleted from the sequence. Reads with identical UMIs were collapsed into a single
706 consensus sequence for each UMI. UMI read groups having a nucleotide diversity score exceeding 0.1 were
707 discarded. Finally, corrected consensus sequence read pairs were assembled into full length sequences with a
708 maximum allowed error rate of 0.2 and p-value threshold of 0.1. All unique sequences that were not
709 represented by at least two raw reads were removed from further analysis and duplicate full-length
710 sequences were discarded. Following pre-processing, sequences were further processed using MIXCR as
711 described above with the computational correction of PCR errors option turned off (-
712 OcloneClusteringParameters=null).

713

714 **Mutation and N-joints**

715 To resolve junctional and N-joint regions, the V, N1, D, N2, and J subregions were defined on the sequences
716 exported using MIXCR. Normalized CDR3 subregion (V, N1, D, N2, J) lengths (median) of clonotypes by B
717 cell subpopulation were calculated. Mutation analysis was performed on the annotated sequences exported
718 using MIXCR excluding N-joint regions. Each mutation was reported at the amino acid level for V and J
719 segments counted per sequence. The median number of mutations per sequence over a given repertoire is
720 reported.

721

722 **Rarefaction plots**

723 In order to explore the relationship between sample size and diversity coverage, rarefaction and
724 extrapolation sampling curves were generated using the iNEXT R package³⁹.

725

726 **Determination of sequence similarity among clones within a repertoire**

727 The Levenshtein distance between all pairwise CDR3 amino acid sequence combinations of identical CDR3
728 amino acids was calculated, and each Levenshtein distance was subsequently normalized by the sequence
729 length of the respective sequence combination. Levenshtein distances were computed using the stringdist
730 package in R⁴⁰.

731

732 **Network construction and analysis**

733 The networks were constructed by representing each unique amino acid CDR3 sequence (clone) as nodes.
734 Clones that were exactly one amino acid substitution, insertion or deletion (Levenshtein distance = 1) apart
735 were connected by edges as previously described⁴¹. An antibody repertoire network is an undirected graph
736 $G = (V, E)$ described as a set of nodes (CDR3 vertices, V) together with a set of connections (similarity
737 edges, E), representing the adjacency matrix A of pairwise Levenshtein distances (LD) between CDR3
738 amino acids.

739 Degrees (number of similar CDR3 sequences to a specific CDR3 sequence) were calculated for each
740 similarity layer LD1 for each CDR3 sequence in each sample. CDR3 with zero degrees that were not similar
741 to any other CDR3 in the network were excluded in order to fit degree distributions. The contribution of
742 expanded clonotypes within a given repertoire consisted of the sum of clonotypes with a degree ≥ 1 on a
743 Levenshtein distance 1 network over the size of the repertoire. The networks were visualized employing
744 Cytoscape or the Fruchterman–Reingold layout and Kamada–Kawai layout algorithms using the igraph R
745 package⁴². For networks based on single cell data concatenated heavy and light chain amino acid CDR3
746 sequences from the same cell were analysed.

747

748 **Single cell transcriptomics and repertoire sequencing**

749 Germ-free mice were either mucosally exposed to 3×10^{10} c.f.u. *E. coli* HA107, systemically exposed to $3 \times$
750 10^8 c.f.u. *E. coli* HA107 or maintained as germ-free controls. Spleens and mesenteric lymph nodes were
751 removed on day 21 and disaggregated to single cell suspensions. Cells were enriched for CD138⁺ plasma
752 cells by magnetic cell sorting. Cells were washed once and resuspended in PBS/0.05% (w/v) BSA. The 10x
753 Genomics platform was used to perform concurrent B cell VDJ repertoire sequencing and single cell 5' gene
754 expression analysis. Prepared libraries were sequenced on an Illumina NovaSeq 6000 (2x150 cycles, paired-
755 end mode).

756

757 **V(D)J immunoglobulin single cell sequencing analysis**

758 *Processing raw sequencing data*

759 The CellRanger software version 3.0.1 was used to process the raw sequencing data produced by the 10x
760 Chromium direct Ig enrichment. The 10x genomics mouse genome GRCm38.93 3.0.0 release was used as
761 reference for the alignments. The “filtered contigs” files were subsequently used for downstream analyses.

762

763 *VDJ annotation of BCR contigs*

764 Following pre-processing, sequences were further analysed using MIXCR v2.1.12 as described above with
765 the computational correction of PCR errors option turned off (-OcloneClusteringParameters=null). VDJ
766 alignment and annotation was performed against C57BL/6J germline gene data. CDR3 regions were defined
767 by MiXCR according to the nomenclature of the Immunogenetics database (IMGT). Clonotypes were
768 defined by 100% amino acid sequence identity of CDR3 regions.

769

770 *Filtering and display of relationships between exposure conditions in BCR contigs and cells*

771 As with bulk Repseq analyses, only productively rearranged clonotypes were used. Cells with one heavy
772 chain contig paired with one light chain contig were kept for downstream analysis. Cells remaining had been
773 checked to have a transcriptomic profile consistent with B-cells (cells with any one of the following
774 markers: CD19, CD138 or the isotype-encoding genes with a positive log-normalized expression level).
775 Given the limited output at single-cell level, repertoire overlap was relaxed from 100% to 90% amino acid
776 identity incorporating a length correction². The relative overlap was normalized for the resulting repertoire
777 size and similarity was represented as hierarchical clustering or multi-dimensional scaling (MDS) plots.

778

779 **Statistical significance**

780 Statistical significance was tested either using Student t-test or the Wilcoxon rank-sum test followed by a
781 Benjamini-Hochberg correction for false discovery rate. Results were considered significant for $p_{adj} < 0.05$.

782

783 **Data availability**

784 The raw files for the datasets generated during this study is available on the SRA bioproject PRJNA625440
785 access number. The pre-processed files (clonotype list and properties) are available on the github repository
786 <https://github.com/Mucosal-Immunology-Bern/Manuscript-microbiota-and-B-cell-repertoire>. The associated
787 codes for the analysis using R packages are to be found in the same github repository.

788

789 **Availability of biological materials**

The bacterial strains for reversible germ-free colonisation can be obtained without restriction from A.J.M
and S.H. following a material transfer agreement with the University of Bern.

790 **SUPPLEMENTARY REFERENCES**

791

792 25 Macpherson, A. J. *et al.* A primitive T cell-independent mechanism of intestinal mucosal IgA responses
793 to commensal bacteria. *Science* **288**, 2222-2226, (2000).

794 26 Rivera, M. C., Maguire, B. & Lake, J. A. Isolation of ribosomes and polysomes. *Cold Spring Harb*
795 *Protoc* **2015**, 293-299, (2015).

796 27 Slack, E. *et al.* Innate and adaptive immunity cooperate flexibly to maintain host-microbiota mutualism.
797 *Science* **325**, 617-620, (2009).

798 28 Tomayko, M. M., Steinel, N. C., Anderson, S. M. & Shlomchik, M. J. Cutting edge: Hierarchy of
799 maturity of murine memory B cell subsets. *J Immunol* **185**, 7146-7150, (2010).

800 29 Greiff, V. *et al.* Quantitative assessment of the robustness of next-generation sequencing of antibody
801 variable gene repertoires from immunized mice. *BMC Immunol* **15**, 40, (2014).

802 30 Krebber, A. *et al.* Reliable cloning of functional antibody variable domains from hybridomas and spleen
803 cell repertoires employing a reengineered phage display system. *J Immunol Methods* **201**, 35-55, (1997).

804 31 Menzel, U. *et al.* Comprehensive evaluation and optimization of amplicon library preparation methods
805 for high-throughput antibody sequencing. *PLoS One* **9**, e96727, (2014).

806 32 Bolotin, D. A. *et al.* MiXCR: software for comprehensive adaptive immunity profiling. *Nat Methods* **12**,
807 380-381, (2015).

808 33 Greiff, V. *et al.* Systems Analysis Reveals High Genetic and Antigen-Driven Predetermination of
809 Antibody Repertoires throughout B Cell Development. *Cell Rep* **19**, 1467-1478, (2017).

810 34 Lefranc, M. P. *et al.* IMGT, the international ImMunoGeneTics database. *Nucleic Acids Res* **27**, 209-212,
811 (1999).

812 35 Shugay, M. *et al.* VDJtools: Unifying Post-analysis of T Cell Receptor Repertoires. *PLoS Comput Biol*
813 **11**, e1004503, (2015).

814 36 Stern, J. N. *et al.* B cells populating the multiple sclerosis brain mature in the draining cervical lymph
815 nodes. *Sci Transl Med* **6**, 248ra107, (2014).

816 37 Khan, T. A. *et al.* Accurate and predictive antibody repertoire profiling by molecular amplification
817 fingerprinting. *Sci Adv* **2**, e1501371, (2016).

818 38 Vander Heiden, J. A. *et al.* pRESTO: a toolkit for processing high-throughput sequencing raw reads of
819 lymphocyte receptor repertoires. *Bioinformatics* **30**, 1930-1932, (2014).

820 39 Hsieh, T., Ma, K. & Chao, A. iNEXT: an R package for rarefaction and extrapolation of species diversity
821 (Hill numbers). *Methods in Ecology and Evolution* **7**, 1451-1456, (2016).

822 40 van der Loo, M. The stringdist package for approximate string matching. *R Journal* **6**, 111-122, (2014).

823 41 Miho, E., Roskar, R., Greiff, V. & Reddy, S. T. Large-scale network analysis reveals the sequence space
824 architecture of antibody repertoires. *Nat Commun* **10**, 1321, (2019).

825 42 Csardi, G. & Nepusz, T. The igraph software package for complex network research. *Interjournal*,
826 *Complex Systems*, 1695, (2006).

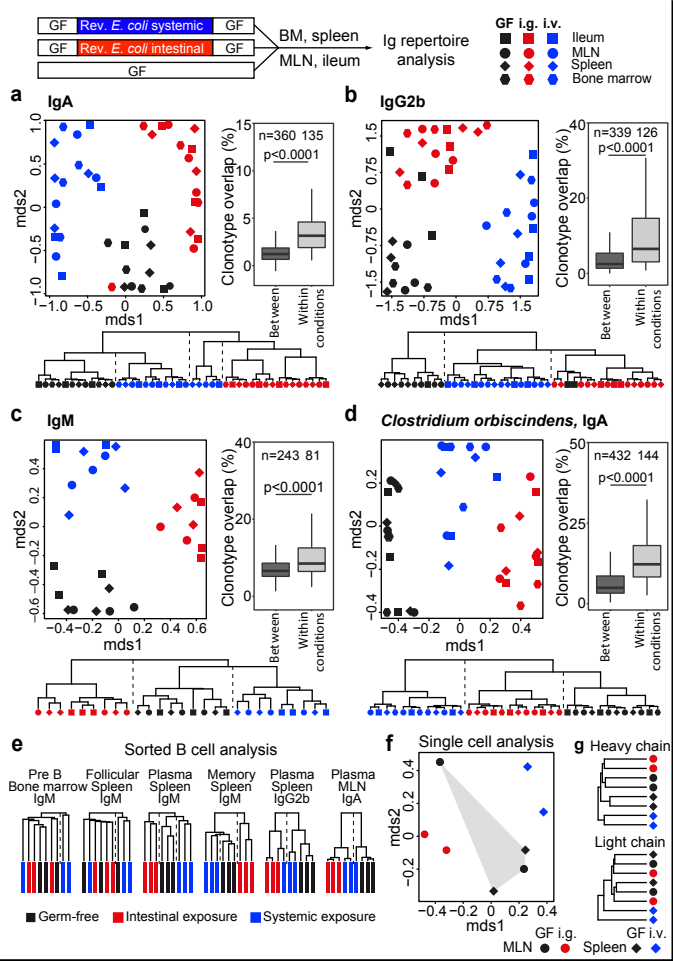


Figure 1

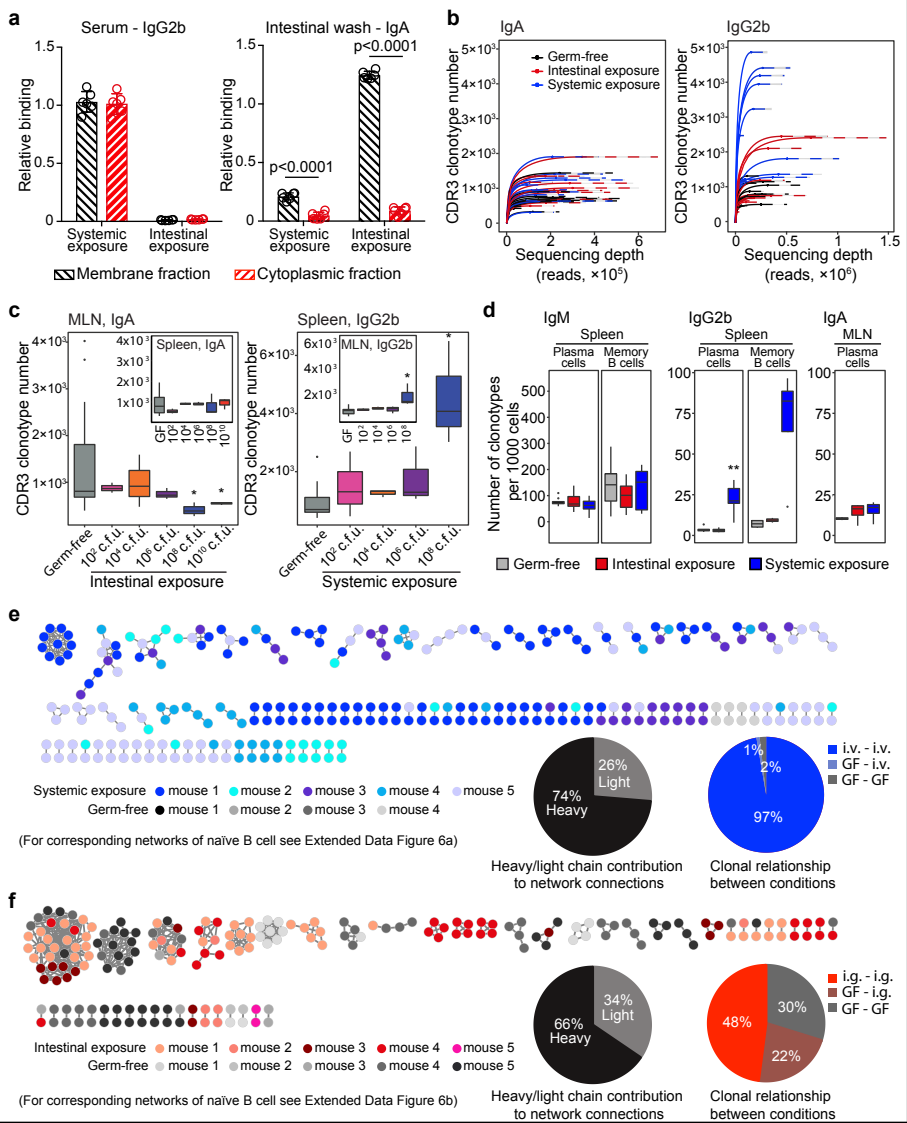


Figure 2

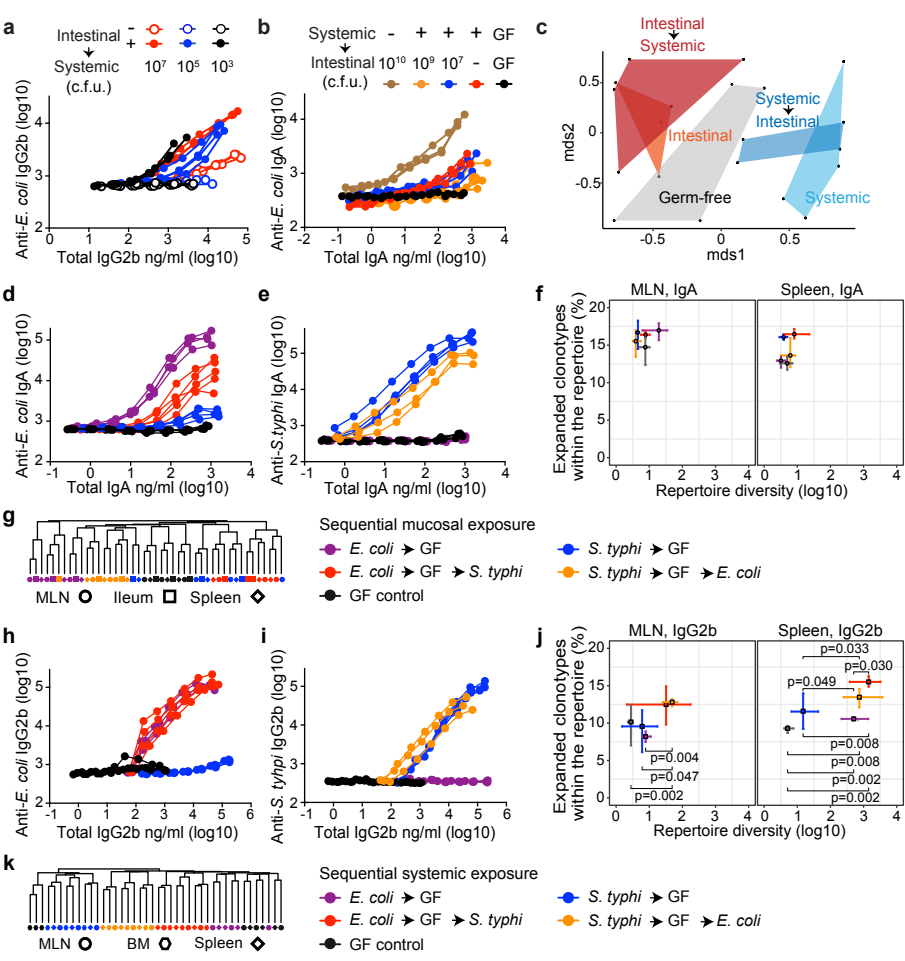


Figure 3